Composites Communications 62 (2026) 102697

Contents lists available at ScienceDirect

Composites Communications

journal homepage: www.elsevier.com/locate/coco

Short Communication

Interphase-engineering by atomic layer deposition of nacre-inspired alumina composites

Talha Nisar [a], Nithin Thonakkara James [a], Laura Grassi Maragno [b], Emeline Chevallier [b], Diego Ribas Gomes [a], Eloho Okotete [a], Subin Lee [a], Christoph Kirchlechner [a], Kaline P. Furlan [a,*]

[a] Karlsruhe Institute of Technology (KIT), Institute for Applied Materials, Kaiserstraße 12, Karlsruhe, 76131, Germany
[b] Hamburg University of Technology (TUHH), Integrated Ceramic-based Materials Systems Group, Denickestraße 15, 21073, Hamburg, Germany

ARTICLE INFO

Keywords:
Nacre-inspired
Bio-inspired composite
Atomic layer deposition
Aluminum oxide
Mechanical properties

ABSTRACT

Nacre, also known as mother of pearl, is a layered brick-and-mortar structure composed of hard mineral platelets and soft organic protein. Found in the inner shells of certain mollusks, this natural architecture has evolved to optimize mechanical properties for the protection of the organism. The unique structured design of nacre and its exceptional mechanical performance have inspired the development of synthetic nacre-like materials. In this work, we introduce a novel approach for fabricating nacre-inspired ceramic composites using atomic layer deposition (ALD) to engineer the interphase, or "mortar", between aligned alumina platelets. ALD, known for its sub-nanometer thickness control and conformal coating capabilities, enables uniform tuning of the interphase thickness from 30 nm up to 120 nm, offering a significant advantage in tailoring the mechanical properties of ceramic-ceramic composites. Our results reveal a direct correlation between ALD-deposited aluminum oxide thickness and enhanced mechanical performance, with increased modulus and hardness observed as the mortar thickens. Three-point bending tests further show that flexural strength is maximized with thicker ALD coatings. *In situ* micromechanical testing reveals crack initiation at surface defects in micro-cantilevers, with cracks effectively deflected by the nacre-inspired architecture. This resultsin an average flexural strength of approximately 400 MPa, achieved without additional heat treatment or sintering. The precision of ALD in creating conformal interphases is critical to the improved structural integrity and performance of the composite, demonstrating its potential asa powerful technique for fabricating high-performance, bio-inspired ceramic composites.

1. Introduction

Nature has long served as a source of inspiration for the development of advanced materials [1]. For the past few decades, researchers in the material science community have been increasingly interested in mimicking natural composites, as studies have revealed remarkable mechanical properties arising from their complex microstructure and geometry, which efficiently distribute stress from the nano-to the macro-scale [2]. One of the most remarkable natural materials is nacre, also known as mother-of-pearl, which exhibits a unique combination of strength, toughness, and low density [3]. To achieve enhanced mechanical performance, the nacre structure relies on two main components: aragonite platelets - "bricks" - that provide strength and stiffness, and a thin organic interlayer - the "mortar" or "binder" - that absorbs energy and prevents damage. Nevertheless, the mechanical performance of nacre is not simply the sum of its constituents' properties as predicted by the rule of mixtures; rather, it arises from synergistic enhancements due to its hierarchical brick-and-mortar structure [4]. Although the individual building blocks of nacre, i.e. calcium carbonate and bio-polymers, are intrinsically brittle and weak, nacre exhibits an unusual combination of strength, stiffness, and toughness that is highly desirable for engineering applications [5,6]. For instance, the fracture toughness (K_{IC}) of nacre is approximately 3.4 MPa$\cdot\sqrt{m}$ [3], which is three to nine times higher than that of monolithic aragonite. This high toughness is achieved through both intrinsic and extrinsic toughening mechanisms, such as crack arrest and energy dissipation via

* Corresponding author.
E-mail address: kaline.furlan@kit.edu (K.P. Furlan).

https://doi.org/10.1016/j.coco.2025.102697
Received 29 July 2025; Received in revised form 17 December 2025; Accepted 28 December 2025
Available online 3 January 2026
2452-2139/© 2026 The Authors. Published by Elsevier Ltd. This is an open access article under the CC BY license (http://creativecommons.org/licenses/by/4.0/).

platelet-platelet sliding events [4,5,7,8]. Furthermore, redistribution of mechanical load occurs through various mechanisms: i) microscopic deformation processes, e.g. plastic or viscoelastic deformation in the mortar phase, and ii) crack deflection at platelets-mortar interfaces. In such microarchitectures, mechanical energy is not concentrated locally but rather dissipated though mechanisms such as platelet sliding and crack deflection, thereby preventing catastrophic failure [9]. Consequently, many high-performance composite materials adopt the brick-and-mortar architecture of nacre to distribute stress across multiple length scales, including nacre-like composites [10], fiber-reinforced composites [11], and various bio-inspired coatings [2].

In the pursuit of nacre-inspired composites, alumina platelets have emerged as the most promising candidate for the "brick" building blocks due to their intrinsic properties such as high aspect ratio, high hardness, high strength, thermal stability, and chemical resistance [12]. The fabrication of nacre-like bio-inspired composites using alumina platelets to create the brick structure has been reported by various research groups employing different methods, including freeze casting, centrifugation, slip casting, hot pressing, laser engraving, and additive manufacturing [13–16]. Some of the most advanced nacre-like composites have demonstrated flexural strengths of up to 400 MPa, elastic moduli ranging from 30 to 50 GPa, and fracture toughness values between 5 and 30 MPa $\sqrt{m}\cdot$ [17–19]. In many of these earlier works, however, the mortar is often polymeric, which limits their application in more demanding environments. This has motivated the recent expansion of the biomimetic approach to material systems beyond nacre-inspired ceramic-polymer composites, including ceramic-ceramic and ceramic-metallic composites [20–22]. Contrary to expectations, a recent review by Bouville et al. [21] showed that ceramic-ceramic composites, such as nacre-like alumina structures, possess excellent resistance to crack propagation - comparable to composites with polymeric or metallic interphases. One of the most significant advantages of alumina-based nacre-like structures is their excellent thermal stability, enabling their use in high-temperature environments where polymers or other materials would degrade. For instance, the high strength and thermal stability of alumina at elevated temperatures make it ideal for components in power plants, industrial furnaces, or aerospace-related applications.

Despite these advancements, a fundamental limitation in current nacre-inspired ceramic composites is the lack of precise control over mortar thickness and uniformity, particularly at the nanoscale. In natural nacre, the organic interlayers are consistently uniform within individual specimens, but different nacre species show thicknesses ranging between 10 and 50 nm. [23]. Moreover, earlier studies have shown that the strength and adhesion of the mortar phase play a crucial role in determining the final mechanical properties of the composite, where an increase in interfacial bonding strength has led to improvements in both modulus and hardness [9,24]. In earlier studies, the mortar phase was often introduced by physical deposition or infiltration [18], while more recent works have focused on functionalization of either the mortar or the platelets to achieve chemical bonding between the two. Nevertheless, existing methods - such as solution-based or sol-gel-based processing for polymer and ceramic mortar infiltration, respectively - struggle to achieve precise thickness control and uniformity over large areas, limiting the ability to fully mimic the structure and properties of natural nacre. Therefore, a significant challenge in the fabrication of nacre-inspired composites is achieving precise control over the thickness of the mortar material while simultaneously ensuring uniform distribution over large areas.

Atomic layer deposition (ALD) offers a powerful solution for the precise engineering of the mortar phase in nacre-like alumina or, more generally, nacre-like ceramic-ceramic composites. ALD is a vapor-phase technique that enables the deposition of ultra-thin, conformal coatings with sub-nanometer-level thickness control. Owing to its self-limiting, surface-controlled reaction behavior, ALD ensures uniform and homogeneous coating of all surfaces accessible to the gaseous precursors [25]. Previous studies have demonstrated the remarkable capabilities of ALD across various fields, including porous materials [26], energy conversion [27] and storage [27], catalysis [28], plasmonics [27,29] and photonics applications [30–33]. Nevertheless, the potential of ALD for systematic interface modification and interfacial engineering in nacre-inspired ceramic-ceramic composites remains largely unexplored. Notably, ALD could enable tunable interphase thickness and, due to its inherent surface chemistry [25], could facilitate the formation of a chemically-bonded interface between the mortar and brick phases, with precisely controlled thickness - potentially mimicking the microstructure observed in natural nacre.

In this study, we present a new approach for the fabrication of nacre-inspired ceramic composites by using ALD to engineer the interphase between aligned alumina platelets. We systematically investigate the effect of ALD-deposited aluminum oxide mortar thickness on the mechanical properties of the composite, assessing modulus, hardness and flexural strength through nanoindentation and three-point bending tests. Additionally, we perform *in situ* micromechanical testing inside a scanning electron microscope (SEM) to examine crack propagation and energy dissipation mechanisms. Our findings reveal that increasing the ALD interphase thickness enhances the modulus, hardness and flexural strength while preserving a hierarchical structure capable of effective crack deflection. The best performance is observed in the composite with a 120 nm-thick interphase, which achieves a flexural strength of 400 MPa without any additional heat treatment or sintering. This work establishes ALD as a viable method for precise interphase engineering and porous materials functionalization, offering new design opportunities for high-performance, bio-inspired ceramic composites.

2. Materials and methods

Alumina platelets, with an average nominal lateral size of 2 μm and an average nominal thickness of 150 nm, were purchased from Qinsai and used as the primary brick material for the nacre-inspired composite. The alumina platelets were aligned by centrifugation, following the protocol reported by Amini [34], where modifications were made to enable the possibility to perform ALD coating of free-standing structures. Initially, 80 mg of the alumina platelets were suspended in deionized (DI) water in a centrifuge tube with a diameter of 300 mm. To ensure a homogeneous dispersion, the mixture was first agitated using a vortex mixer and then ultrasonicated for 10 min. Following the mixing process, the alumina suspension was subjected to centrifugation using a centrifuge (Megafuge 16, Thermo Fisher Scientific Inc. USA) at 5500 rpm (equivalent to 4974g) for 25 min. After centrifugation, the supernatant was carefully removed using an Eppendorf pipette and the resultant thin layer of alumina platelets was left to dry in open air at room temperature. The substrate used during the centrifugation process was a polytetrafluoroethylene (PTFE) plate covered with Kapton™ tape, for easy separation of the platelet layer from the substrate after drying.

Once dried, the samples were transferred to an ALD reactor chamber (GEMStar XT, Arradiance, USA) to generate the aluminum oxide coating as the mortar material. The ALD chamber was preheated and maintained at a temperature of 150 °C, with a steady flow of 10 sccm of nitrogen as a carrier gas, where the samples were kept for 3 h to ensure removal of any residual moisture before the deposition process began. The precursors used for the aluminum oxide deposition were trimethylaluminum (TMA, STREM-Ascensus Specialties) and ultrapure water. The ALD cycles consisted of a sequence of (0.4–60)-90-(0.4–60)-90 s of (pulse-hold)-purge-(pulse-hold)-purge for TMA and water, respectively. For measuring the deposited thicknesses, reference silicon wafers (<100>-oriented, Si-Mat Silicon Materials) were placed inside the reactor chamber close to the centrifuged samples, and then analyzed by spectroscopic ellipsometry with an incident angle of 70° (SENpro, Sentech GmbH, Germany). For this purpose, Cauchy model was used to fit the spectra obtained from the ALD coatings and the growth per cycle (GPC) was determined to be 1.6 Å. The determined GPC in this study is slightly

higher than the usual value reported work for planar films (1.1–1.3 Å), but consistent with our earlier works on coating of polymeric templates for the fabrication of 3D photonic structures [30–33]. The ALD cycle was repeated until the desired thicknesses of 30, 60, 90 and 120 nm were achieved. The ALD interphase thickness was systematically varied from 30 to 120 nm. The overview of the experimental procedure for samples' fabrication is shown in Fig. 1.

The alignment of the platelets was assessed by analyzing the samples' cross section using SEM (Supra 55 VP, Carl Zeiss, Germany) with an applied low accelerating voltage of 3 kV at a working distance of around 5 mm. For the SEM measurements, cross-section surface of the nacre-like composites was polished using an ion-milling system (Leica, Microsystems, Germany) equipped with three Ar^+ guns. The polishing was done at an acceleration voltage of 7 kV, and a current of 3 mA for 3 h.

To assess the impact of the ALD coatings on the indentation hardness and modulus at the microscale, nanoindentation (G200, Agilent, USA) was performed on the surface of the coated samples using a Berkovich tip (Synton MDP, Switzerland). The tests were carried out in continuous stiffness measurement (CSM) mode, utilizing an oscillation amplitude of 2 nm at a frequency of 45 Hz. The indents, 25 indentations per sample, were performed at a maximum depth of 2.1 μm, which was selected based on a preliminary indentation size effect study, detailed in the Supplementary Information file (Fig. S1). The Young modulus (E) was determined from harmonic contact stiffness data recorded during the loading segment of the force-displacement curve. The reported *E* values correspond to the stable region of the stiffness-displacement curve, where the stiffness remained constant before the first detectable failure event. To further characterize the mechanical properties such as flexural strength, the nacre-like alumina composites were cut into rectangular bars. The three-point bending tests were conducted using a nanoindenter (G200, Agilent, USA) equipped with a wedge tip, with a span distance of 840 μm (see Fig. S2 in the supplementary information). The dimensions of the rectangular bars were measured using an optical profilometer (ALICONA G4 infinite Focus, Austria) to ensure the correct calculation of the mechanical properties' values.

Additionally, quantitative bending tests using micro cantilevers were conducted on the nacre-inspired composite that obtained the best results regarding flexural strength, namely the sample ALD-coated with 120 nm of aluminum oxide, to provide further insight into the mechanical behavior of the fabricated composite. For this purpose, 15 microcantilevers with widths and thicknesses between 14 and 15 μm and lengths maintained at 5 times the thickness were fabricated using a combination of femtosecond pulsed laser (fs-laser) and focused ion beam milling (FIB) (Crossbeam 550L, Carl Zeiss AG, Germany). First, the composite material was ablated with the fs-laser set to 40 % of the maximum power (29 MW of pulse peak power), 300 mm/s scan speed, and 100 kHz frequency to produce the desired geometry at the edge of the free-standing surface of a 2 × 2 mm macro sample. Then, undercuts were used to make the cantilevers free-standing using the same fs-laser milling conditions. A final step involved polishing the side walls of the cantilevers using a Ga^+ FIB at an acceleration voltage of 30 kV with a beam current of 30 nA and a dose of 50 nC/m^2 to remove possible damage layers and beam taper introduced by the fs-laser. *In situ* SEM cantilever bending tests were performed on these cantilevers inside an SEM (Merlin, Carl Zeiss AG, Germany) using a PI89 indenter (Hysitron, Bruker, USA) with a 20 μm diamond wedge tip (Synton-MDP AG, Switzerland) attached. The experiments were conducted in displacement-controlled mode at a rate of 100 nm/s to monitor the material's response.

3. Results and interpretation

The microstructural morphology of the samples analyzed via cross-section SEM imaging (Fig. 2), distinctly showcases the stacked, brick-like arrangement, which is crucial for mimicking the hierarchical architecture of nacre. As previous reports [15,34] also pointed out that higher platelet's alignment is associated with better load transfer and mechanical integrity, a quantitative analysis of platelet alignment is shown in Fig. 2c, where the x-axis represents the angle relative to the horizontal and the y-axis denoted the frequency of platelets at each angle. The results indicate a preferential platelet orientation parallel to the substrate (Fig. 2c), confirming that the centrifugation process successfully aligned the platelets. The alignment level is comparable to earlier reports where platelets were also aligned by centrifugation [34] or other methods [35,36], yet lower than in natural nacre [5]. A closer look into the ion-polished cross-section clearly indicates the presence of misaligned platelets (Fig. 2b). These residual misalignments and irregular shapes contribute to the high porosity of the final structure, which is visualized in the ion-milled cross-section in Fig. 2b. An assessment of the porosity by image analysis, conducted on five images, yielded an average of 25.4 % with a standard deviation of 1.9 %. A potential future reduction of porosity is expected to enhance the mechanical performance of the composite, as porosity acts as a stress concentrator, leading to premature failure under mechanical loading. Thus, further process optimization focusing on misalignments and structural density, might lead to improved mechanical properties. Nevertheless, as we wanted to study the impact of the ALD coating thickness (30–120 nm) on the mechanical properties, we did not focus on optimizing the self-assembly process, but rather used the same initial self-assembly condition, already reported in other studies focusing on self-assembly, for all investigated samples.

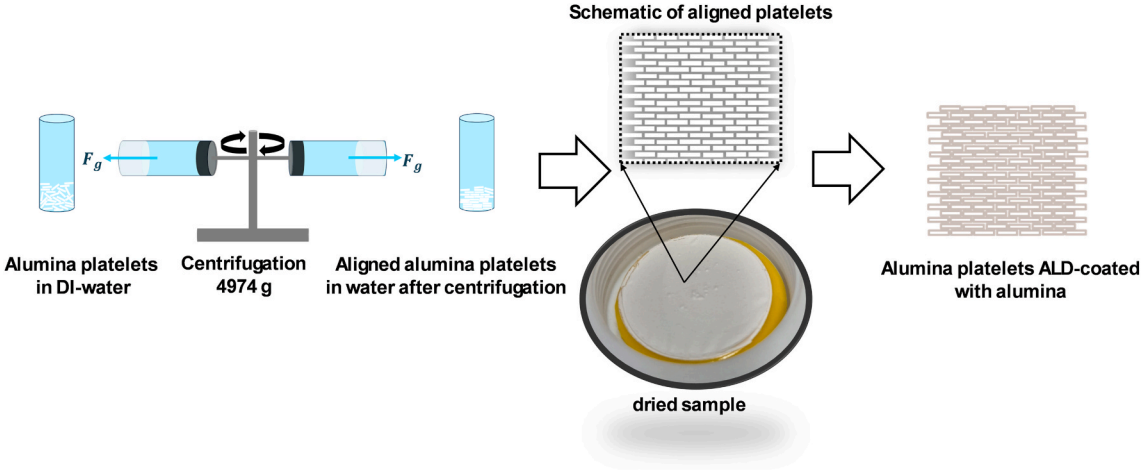

Fig. 1. Schematic drawing shows an overview of the fabrication process involving centrifugation of alumina platelets as brick material to form the to-be-coated skeleton, followed by ALD coating of aluminum oxide to serve as the mortar material resulting in ceramic-ceramic nacre-like composites.

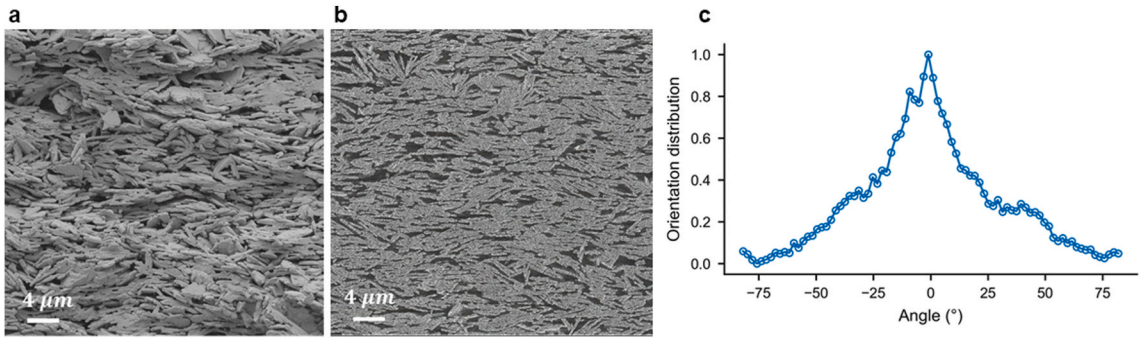

Fig. 2. SEM cross-section of ALD-processed nacre-inspired sample with 90 nm Al_2O_3 mortar layer; a) freshly cut with a razor blade without further polishing; and b) after fine polishing via ion-milling. c) Normalized degree of alignment of the centrifuged platelets extracted from SEM image (Fig. 2b) using ImageJ software and the directionality plugin.

After understanding the microstructure (alignment of the platelets and porosity) of the nacre-inspired composite, we now focus on the role of ALD processed mortar in further improving the mechanical properties of the nacre-inspired sample. Despite the reduced interphase thickness, the impact of ALD-generated interphase in the mechanical properties of the composites is substantial (Fig. 3), with both Young's modulus and indentation hardness increasing with ALD-coating thickness.

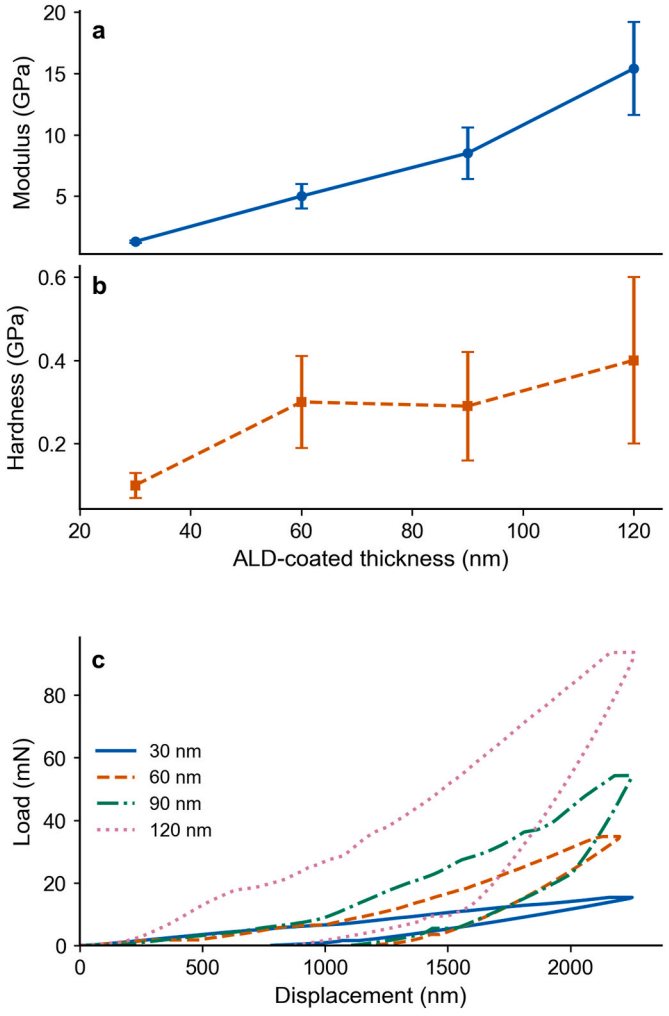

Fig. 3. Mechanical properties of the ALD-coated nacre-inspired composites with varying thicknesses of the ALD-coated aluminum oxide as the interphase: a) Indentation modulus, b) Hardness, c) representative load-displacement curves from each sample.

Furthermore, analysis of the load–displacement curves (Fig. 3c) confirms that the slope of the loading segment becomes progressively steeper with increasing thickness of the ALD interphase. This enhancement overcomes the adverse effects of the ≈25 % porosity presents between the alumina platelets. Specifically, a thicker ALD interphase reduces the gaps between platelets, potentially leading to more efficient stress transfer between the stiff alumina platelets (see Fig. S5). By reducing the compliance associated with the porous regions, the thicker interphase enables the platelets skeleton to contribute more effectively to resisting the applied load. Consequently, the composite benefits from enhanced mechanical interlocking, an effective reduction in porosity, and overall higher volumetric fraction of the mortar phase, all of which contribute to its increased resistance to deformation. These findings confirm what is well-documented in previous studies on nacre-like materials, where interphase properties significantly influence mechanical performance [15,35].

In our case, ALD forms a chemically bonded interface, which is hypothesized to also improve interfacial strength due to efficient load transfer, resulting in the observed increase in mechanical properties. However, the precise characterization of the interfacial strength of the ALD-platelet for quantitative and comparative analysis was not conducted in the present work; it remains as an open question that would be a subject for future studies. Previous studies on ceramic-ceramic nacre-inspired composites produced using various methods have reported modulus values an order of magnitude higher [37,38], which could be linked to post-processing steps, such as hot pressing. In the present study, the maximum temperature used during processing was 150 °C implying that the results obtained here reflect the condition with no post-processing, i.e., right after ALD, so that no pressure or thermal post-processing is applied. Therefore, the authors foresee room for improvement in future investigations dealing with post-processing of ALD-based bio-inspired composites.

Three-point bending tests further validated the role of ALD coating interphase thickness in enhancing mechanical performance (Fig. 4). The results show that the flexural strength increased from approximately 15 MPa for a 30 nm layer to ≈110 MPa for 120 nm.

This trend is consistent with previous work on nacre-inspired composites, where thicker interphase in nacre-like ceramic-polymeric composites improved platelets-to-platelets connection by providing more interface material to fill the gaps between the platelets and enhance load-bearing capacity, leading to higher flexural strength [39]. Even though a direct correlation between a polymeric mortar and a ceramic mortar cannot be made due to the very different material characteristics, we associate the higher flexural strength with enhanced platelets-to-platelets connection, as in the former composites, and thus, enhanced load-bearing capacity. The flexural strength of natural hydrated nacre has been reported to values around 80 MPa [21], which is comparable to our obtained values from three-point bending tests.

Conversely, the average maximum surface strain that the material

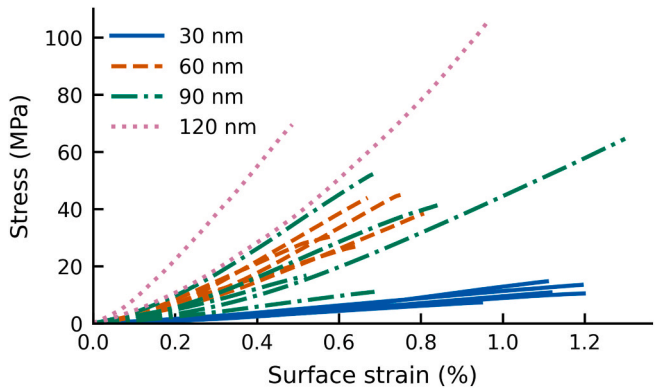

Fig. 4. Three-Point Bending test results of nacre-inspired composites with varying ALD interphase thicknesses.

can endure during a three-point bending test decreases from 1.2 % to 0.3 % (see Fig. S4b), suggesting a transition toward brittle behavior as the interphase thickens, which is not surprising for a purely ceramic mortar. This can be attributed to the restriction of platelet sliding, a hallmark energy dissipation mechanism in nacre-like materials. Composites with thinner mortar layers can accommodate the slight sliding of platelets during deformation, enabling the material to absorb more strain energy prior to fracture, leading to greater strain values. The aforementioned sliding mechanism is restricted in composites with thicker mortar layers, resulting in a more brittle response. The maximum strain before failure in the bending test in previous reports of ceramic-ceramic nacre-inspired composite falls in the range between 0.2 and 0.6 % [36,38,40], which is consistent with our lowest values for thicker ALD coatings. Here, an intrinsic advantage of conformally coated amorphous ALD-based aluminum oxide mortars is hypothesized. Recent groundbreaking work by Frankberg et al. [41] demonstrates room temperature ductility for aluminum oxide amorphous ALD thin films, reaching elongations up to 100 %. Nevertheless, unlike this report, here the ALD films are "restrained" by the surrounding platelets.

To gain more insight into the toughening mechanism of the nacre-like alumina composites fabricated in this study, micro cantilevers were prepared for the composite with the highest flexural strength, i.e. the one with 120 nm mortar thickness. Fig. 5 shows representative results from the *in-situ* SEM micro cantilever experiment. The cantilever with the wedge indenter used to apply load is seen in Fig. 5a and 5b shows the load-displacement plot derived from the test. The beginning of the test is characterized by linear elastic deformation until the maximum load of 3.5 mN at point ***c***. As the test continues, the load drops, indicating crack initiation and subsequent propagation as observed in Fig. 5b and corresponding SEM snapshots (Fig. 5c–g). For a video of the *in-situ* testing, please refer to supplementary Video 1. Similar results were seen in all the tested micro cantilevers, indicating the absence of catastrophic failure after crack initiation. A detailed look at the test shows that the crack is initiated at a critical defect on the surface of the cantilever (Fig. 5c). This was also the case for the other tested cantilevers (15 in total), where cracks typically initiated from regions with pores or platelet misalignment. Upon initiation, the crack grows in a stable manner, deflecting along paths of lower resistance (weak interfaces) between the platelets and the mortar. In situ scanning electron microscopy (SEM) bending tests show crack deflection along interfaces, observed within the SEM chamber during loading This crack deflection mechanism mimics the one observed in natural nacre, and is expected to enhance fracture toughness by effectively releasing stress and expanding the plastic zone, owning to the nacre-like architecture with ALD-based mortars.

Unlike the behavior of traditional ceramics, which often fail catastrophically upon crack initiation, our composite presents a non-catastrophic failure behavior as crack propagation was successfully observed in most cases. The improved properties arise due to the nacre-like layered structure, formed by the aligned alumina platelets as bricks and the ALD-coated binder as mortar. This indicates that the fabricated ALD-based nacre-like composite is effective in enhancing fracture toughness via multiple crack deflection along the brick-mortar interfaces. Crack deflection has been previously reported as a typical toughening mechanism in such nacre-like composite materials [42,43]. Our micro cantilever fracture tests show an average flexural strength (σ_f) of 393.2 ± 83.3 MPa (mean value and standard deviation of 15 tests),

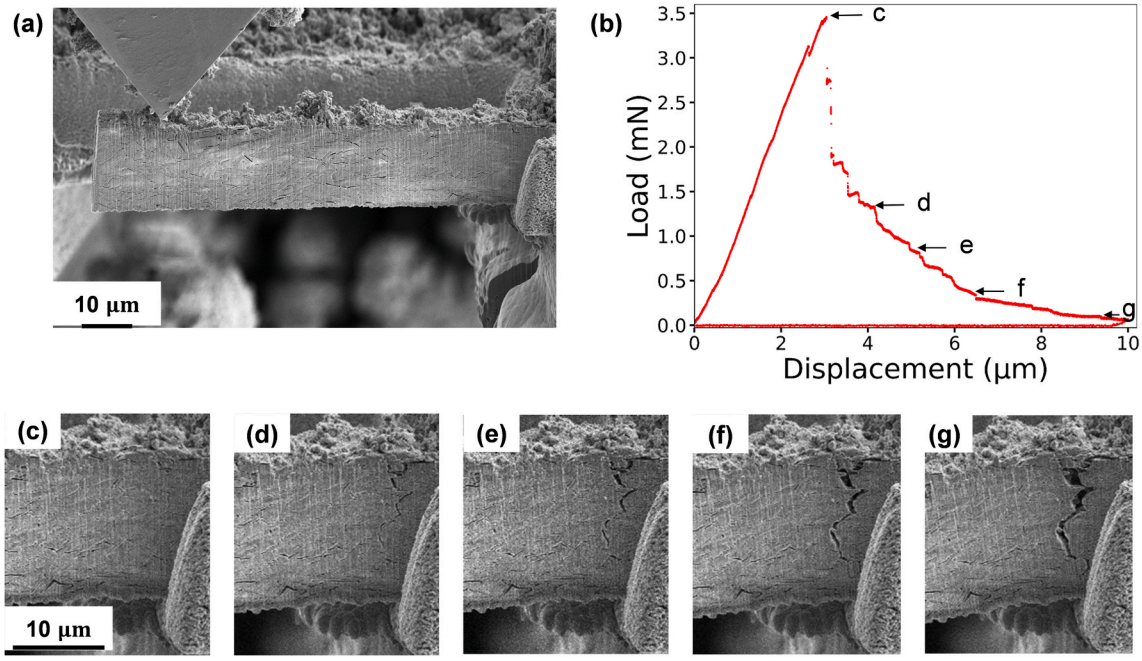

Fig. 5. SEM image of the *in-situ* test setup showing the cantilever and the wedge indenter in SEM chamber during loading. (b) The corresponding load-displacement plot obtained from one exemplary experiment. (c–g) SEM snapshot corresponding to a crack initiation and propagation event during loading showing clear crack deflection.

which is significantly higher than that of conventional ceramics of similar composition without any heat treatment or post processing. The difference in the flexural strength between the *ex-situ* three-point bending test (Fig. 4) and the *in situ* micro-bending test (Fig. 5) is primarily due to a defect sampling effect in the mechanical testing, which is known and expected [44,45]. At the micro-scale, samples show higher strength values due to a reduced number of flaws within the cantilever. In larger volumes, the statistical likelihood of containing a critical defect (e.g., microcracks or voids) which act as stress concentrators, increases. In contrast, fs-laser milled samples, being substantially smaller, contain fewer critical defects, resulting in higher measured strengths. Additionally, the presence of steep strain gradients in thin cantilevers might change the apparent strength [46,47].

4. Discussion

The enhanced mechanical performance (interface thickness dependent) of ALD processed nacre inspired samples can be explained by analyzing the underlying deformation and toughening mechanisms at different scales: i) In situ SEM bending tests (shown in Fig. 5) indicate that cracks propagate along the platelet-mortar interface, instead of the hard alumina platelets. This crack deflection mechanism significantly increases the fracture energy by increasing the crack path. Furthermore, bridging is also visible which further supports energy dispersion during the crack propagation. ii) The alignment of the platelets via centrifugation is also hypothesized to contribute to the enhancement of mechanical performance, by stress redistribution across the sample at platelet interfaces. This alignment induced load redistribution resembles the unique design of natural nacre. iii) The thin ALD processed interface acts as compliant mortar around the alumina platelets. With thinner mortar layers, the composite bear shear deformation and on the other hand, thicker mortar layer, causes improved load transfer.

These mechanisms collectively contribute to enhancing mechanical performance at different scales: nanoscale interface compliance, microscale platelet alignment and crack deflection, as well as bridging at multi-scales enable the ALD processed nacre inspired sample to attain high strength even without post processing.

A wide range of flexural strengths has been reported for ceramic-ceramic nacre-like composites fabricated using different processing techniques and material combinations. For instance, nacre-inspired structure fabricated via Magnetically-Assisted Slip Casting (MASC) combined with transient liquid phase sintering, using alumina platelets as the brick material and aluminum borate as the mortar, achieved flexural strengths of up to 300 MPa [37] after sintering at 1400 °C for 1 h and pressed at 60 MPa. In a related study from the same group, Hortense et al. utilized the same processing route to fabricate nacre-like composites keeping the same brick material while using silica or alumina bridges as the mortar, reporting strengths of up to 600 MPa [36], but only after heat treatment at 1000–1500 °C for 30 min and compressed up to 60 MPa. Alternatively, Bouville et al. employed ice-templating to create a nacre-like structure using alumina platelets reinforced with a mortar made of alumina nanoparticles (≈100 nm) and silica-calcia liquid-phase precursors (≈20 nm), resulting in flexural strengths of up to 420 MPa. To achieve such, the samples were hot-pressed at 1500 °C for 30 min, 100 MPa [38]. Similarly, Koen et al. used Spark Plasma Sintering (SPS) to fabricate a nacre-inspired composite with alumina platelets as the brick material and sintered alumina bridges as the mortar (sintered at 1200–1400 °C, pressed at 50–70 MPa), yet reporting a maximum flexural strength of 140 MPa [40]. To put our obtained results into perspective, we compared the mechanical performance of our ALD processed nacre inspired composite with previously reported bioinspired composites fabricated by different methods, at different process temperature and employing different brick and mortar combinations, including ceramics, polymers and metals (see Table 1).

We emphasize that in this study, a nacre-inspired composite was synthesized using aligned alumina platelets as the brick material and ALD-deposited aluminum oxide as the mortar, processed at a low temperatures of only 150 °C. The resulting composite achieved an average flexural strength of 87 MPa from macroscopic three-point bending tests and up to 390 MPa in *situ* SEM micro-cantilever fracture tests. The significantly higher strength observed at the microscale point out to the importance of the self-assembly process optimization and reduction of defects, since the *in-situ* bending tests showed that all samples had their failure starting at a pore or pre-existing crack. Nevertheless, unlike previously reported studies, the ALD fabrication strategy did not involve any sintering, hot pressing or pressure-assisted sintering, highlighting the unique and remarkable capability of ALD for processing and further development of bio-inspired composites.

5. Conclusion

This study demonstrates a novel approach for fabricating nacre-inspired ceramic-ceramic composites using ALD to engineer and precisely control the interphase, or "mortar", between aligned alumina platelets. By tuning the ALD-deposited aluminum oxide interphase thickness from 30 to 120 nm, we achieved significant improvements in mechanical properties – including increased indentation modulus, hardness, and flexural strength – while preserving the nacre-like architecture capable of deflecting cracks.

Notably, these performance gains were obtained without any high-temperature sintering, hot pressing, or pressure-assisted post-processing, highlighting the capability of ALD as a low-temperature, conformal

Table 1
Comparison of mechanical properties of nacre-inspired composites fabricated by various methods using different brick and mortar materials.

Fabrication method	Brick material	Mortar material	Process temp. (° C)	Young modulus (GPa)	Maximum flexural strength (MPa)	Ref.
Centrifugation + ALD	Al_2O_3	Al_2O_3	150	15	393	This work
Layer by layer assembly	$CaHPO_4.2H_2O$	Sodium alginate	Room temp.	19	275	[39]
Laser engraving	SiO_2	Polyurethane	Room temp.	1	20	[48]
Freeze casting	SiOC	Graphene	1600	100	63	[49]
Freeze casting + Field Assisted Sintering (FAST)	Al_2O_3	Silica (SiO_2) and calcia (CaO)	1500	290	420	[38]
Freeze casting	Al_2O_3	Copper	Room temp.	116	278	[50]
Freeze casting	Al_2O_3	Nickel	1000	150	235	[51]
Natural nacre	Aragonite ($CaCO_3$)	Proteins	–	70	170	[5]
Magnetically Assisted Slip Casting + Hot pressing	Al_2O_3	Aluminum borate ($9Al_2O_3{\cdot}2B_2O_3$)	1200-1400 under 60 MPa pressure	305	300	[37]
Magnetically Assisted Slip Casting	Al_2O_3	SiO_2	1000–1500	60	650	[36]
Spark Plasma Sintering (SPS)	Al_2O_3	Al_2O_3 sintered bridges	1200–1500	Not measured	140	[40]
Thermal spray	Al_2O_3	Epoxy	Room temp.	Not measured	240	[52]

coating technique for the design of advanced structural composites. This sets our method apart from conventional approaches that typically rely on high-energy processing.

While the current results already demonstrate excellent performance, especially at the microscale (up to approximately 390 MPa flexural strength), future investigations may explore selective post-processing strategies, such as low-temperature annealing or mild densification, to further reduce porosity, enhance interfacial bonding, or tailor properties for specific application requirements.

Overall, this work establishes ALD as a powerful and versatile tool for the bottom-up fabrication of bio-inspired, high-performance ceramic composites, and opens new pathways toward scalable, temperature-controlled design of layered structural materials.

CRediT authorship contribution statement

Talha Nisar: Writing – original draft, Visualization, Methodology, Investigation, Formal analysis, Data curation. **Nithin Thonakkara James:** Data curation, Investigation, Writing – review & editing. **Laura Grassi Maragno:** Writing – review & editing, Validation, Investigation, Formal analysis. **Emeline Chevallier:** Investigation. **Diego Ribas Gomes:** Writing – review & editing, Validation, Software, Investigation. **Eloho Okotete:** Writing – review & editing, Visualization, Investigation, Formal analysis. **Subin Lee:** Writing – review & editing, Formal analysis. **Christoph Kirchlechner:** Writing – review & editing, Supervision, Resources, Project administration, Funding acquisition. **Kaline P. Furlan:** Writing – review & editing, Supervision, Resources, Project administration, Methodology, Funding acquisition, Data curation, Conceptualization.

Declaration of competing interest

The authors declare the following financial interests/personal relationships which may be considered as potential competing interests: Kaline P. Furlan reports financial support was provided by German Research Foundation. If there are other authors, they declare that they have no known competing financial interests or personal relationships that could have appeared to influence the work reported in this paper.

Acknowledgement

The authors thank the German Research Foundation (Deutsche Forschungsgemeinschaft, DFG) for their financial support (Grant no: PA3765/4-1).

Appendix A. Supplementary data

Supplementary data to this article can be found online at https://doi.org/10.1016/j.coco.2025.102697.

Data availability

Data will be made available on request.

References

[1] R.T. Kapoor, M. Rafatullah, M. Qamar, M. Qutob, A.M. Alosaimi, H.S. Alorfi, M. A. Hussein, Review on recent developments in bioinspired-materials for sustainable energy and environmental applications, Sustainability 14 (2022).
[2] M.A. Meyers, P.Y. Chen, A.Y.M. Lin, Y. Seki, Biological materials: structure and mechanical properties, Prog. Mater. Sci. 53 (2008) 1–206.
[3] J. Sun, B. Bhushan, Hierarchical structure and mechanical properties of nacre: a review, RSC Adv. 2 (2012) 7617–7632.
[4] Y. Zhang, M. Bartosik, S. Brinckmann, S. Lee, C. Kirchlechner, Toughening nitride hard coatings by deflecting cracks along grain boundaries, Mater. Sci. Eng., A 935 (2025).
[5] A.P. Jackson, J.F. V V, R.M. T, The mechanical design of nacre, Proc. R. Soc. Lond. B Biol. Sci. 234 (1988) 415–440.
[6] M. Grossman, F. Bouville, F. Erni, K. Masania, R. Libanori, A.R. Studart, Mineral nano-interconnectivity stiffens and toughens nacre-like composite materials, Adv. Mater. 29 (2017).
[7] F. Barthelat, H. Tang, P.D. Zavattieri, C.M. Li, H.D. Espinosa, On the mechanics of mother-of-pearl: a key feature in the material hierarchical structure, J. Mech. Phys. Solid. 55 (2007) 306–337.
[8] X.L. Peng, S. Lee, J. Wilmers, S.H. Oh, S. Bargmann, Orientation-dependent micromechanical behavior of nacre: in situ TEM experiments and finite element simulations, Acta Biomater. 147 (2022) 120–128.
[9] U.G.K. Wegst, H. Bai, E. Saiz, A.P. Tomsia, R.O. Ritchie, Bioinspired structural materials, Nat. Mater. 14 (2015) 23–36.
[10] W. Gao, M. Wang, H. Bai, A review of multifunctional nacre-mimetic materials based on bidirectional freeze casting, J. Mech. Behav. Biomed. Mater. 109 (2020).
[11] L. Lassila, F. Keulemans, P.K. Vallittu, S. Garoushi, Characterization of restorative short-fiber reinforced dental composites, Dent. Mater. J. 39 (2020) 992–999.
[12] X. Teng, H. Liu, C. Huang, Effect of Al2O3 particle size on the mechanical properties of alumina-based ceramics, Mater. Sci. Eng., A (2007) 452–453, 545–51.
[13] H. Bai, F. Walsh, B. Gludovatz, B. Delattre, C. Huang, Y. Chen, A.P. Tomsia, R. O. Ritchie, Bioinspired hydroxyapatite/poly(methyl methacrylate) composite with a nacre-mimetic architecture by a bidirectional freezing method, Adv. Mater. 28 (2016) 50–56.
[14] N. Meng, L. Bo, C. Yali, X. Huaqiang, Nacre-inspired Ti (C, N)/Al–Cu composites with high damage tolerance and wear resistance prepared by freeze and squeeze casting, J. Mater. Res. Technol. 26 (2023) 8111–8123.
[15] H. Zhao, Z. Yang, L. Guo, Nacre-inspired composites with different macroscopic dimensions: strategies for improved mechanical performance and applications, NPG Asia Mater. 10 (2018) 1–22.
[16] B.F. Winhard, P. Haida, A. Plunkett, J. Katz, B. Domènech, V. Abetz, K.P. Furlan, G. A. Schneider, 4D-printing of smart, nacre-inspired, organic-ceramic composites, Addit. Manuf. 77 (2023).
[17] M.E. Launey, E. Munch, D.H. Alsem, H.B. Barth, E. Saiz, A.P. Tomsia, R.O. Ritchie, Designing highly toughened hybrid composites through nature-inspired hierarchical complexity, Acta Mater. 57 (2009) 2919–2932.
[18] B.C. Cui, J. Li, Y.H. Lin, Y. Shen, M. Li, X.L. Deng, C.W. Nan, Polymer-infiltrated layered silicates for dental restorative materials, Rare Met. 38 (2019) 1003–1014.
[19] Y. Bu, X. Wang, X. Bu, Z. Mao, Z. Chen, Z. Li, F. Hao, J.C. Ho, J. Lu, Self-assembling nacre-like high-strength and extremely tough polymer composites with new toughening mechanism, J. Mater. Sci. Technol. 136 (2023) 236–244.
[20] A.R. Studart, Additive manufacturing of biologically-inspired materials, Chem. Soc. Rev. 45 (2016) 359–376.
[21] F. Bouville, Strong and tough nacre-like aluminas: process-structure-performance relationships and position within the nacre-inspired composite landscape, J. Mater. Res. 35 (2020) 1076–1094.
[22] F. Libonati, M.J. Buehler, Advanced structural materials by bioinspiration, Adv. Eng. Mater. 19 (2017).
[23] K.S. Katti, B. Mohanty, D.R. Katti, Nanomechanical properties of nacre, J. Mater. Res. 21 (2006) 1237–1242.
[24] F. Mammeri, E. Le Bourhis, L. Rozes, C. Sanchez, Mechanical properties of hybrid organic-inorganic materials, J. Mater. Chem. 15 (2005) 3787–3811.
[25] S.M. George, Atomic layer deposition: an overview, Chem. Rev. 110 (2010) 111–131.
[26] M. Knez, K. Nielsch, L. Niinistö, Synthesis and surface engineering of complex nanostructures by atomic layer deposition, Adv. Mater. 19 (2007) 3425–3438.
[27] M. Liu, X. Li, S.K. Karuturi, A.I.Y. Tok, H.J. Fan, Atomic layer deposition for nanofabrication and interface engineering, Nanoscale 4 (2012) 1522–1528.
[28] C. Hedrich, N.T. James, L.G. Maragno, V. de Lima, S.Y.G. González, R.H. Blick, R. Zierold, K.P. Furlan, Enhanced photocatalytic properties and photoinduced crystallization of TiO2-Fe2O3 inverse opals fabricated by atomic layer deposition, ACS Appl. Mater. Interfaces 16 (2024) 46964–46974.
[29] A.M. Schwartzberg, D. Olynick, Complex materials by atomic layer deposition, Adv. Mater. 27 (2015) 5778–5784.
[30] R.J. Gehensel, R. Zierold, G. Schaan, G. Shang, A.Y. Petrov, M. Eich, R. Blick, T. Krekeler, R. Janssen, K.P. Furlan, Improved thermal stability of zirconia macroporous structures via homogeneous aluminum oxide doping and nanostructuring using atomic layer deposition, J. Eur. Ceram. Soc. 41 (2021) 4302–4312.
[31] K.P. Furlan, E. Larsson, A. Diaz, M. Holler, T. Krekeler, M. Ritter, A.Y. Petrov, M. Eich, R. Blick, G.A. Schneider, I. Greving, R. Zierold, R. Janßen, Photonic materials for high-temperature applications: synthesis and characterization by X-ray ptychographic tomography, Appl. Mater. Today 13 (2018) 359–369.
[32] G. Shang, K.P. Furlan, R. Zierold, R.H. Blick, R. Janßen, A. Petrov, M. Eich, Transparency induced in opals via nanometer thick conformal coating, Sci. Rep. 9 (2019).
[33] G. Shang, K.P. Furlan, R. Janßen, A. Petrov, M. Eich, Surface templated inverse photonic glass for saturated blue structural color, Opt. Express 28 (2020) 7759.
[34] Amini A, Khavari A, Barthelat F and Ehrlicher A J MATERIALS SCIENCE Centrifugation and Index Matching Yield a Strong and Transparent Bioinspired Nacreous Composite.
[35] M. Grossman, F. Bouville, K. Masania, A.R. Studart, Quantifying the role of mineral bridges on the fracture resistance of nacre-like composites, Proc. Natl. Acad. Sci. U. S. A. 115 (2018) 12698–12703.
[36] H. Le Ferrand, F. Bouville, T.P. Niebel, A.R. Studart, Magnetically assisted slip casting of bioinspired heterogeneous composites, Nat. Mater. 14 (2015) 1172–1179.

[37] P.I.B.G.B. Pelissari, F. Bouville, V.C. Pandolfelli, D. Carnelli, F. Giuliani, A.P. Luz, E. Saiz, A.R. Studart, Nacre-like ceramic refractories for high temperature applications, J. Eur. Ceram. Soc. 38 (2018) 2186–2193.
[38] F. Bouville, E. Maire, S. Meille, B. Van De Moortèle, A.J. Stevenson, S. Deville, Strong, tough and stiff bioinspired ceramics from brittle constituents, Nat. Mater. 13 (2014) 508–514.
[39] H.L. Gao, S.M. Chen, L.B. Mao, Z.Q. Song, H Bin Yao, H. Cölfen, X.S. Luo, F. Zhang, Z. Pan, Y.F. Meng, Y. Ni, S.H. Yu, Mass production of bulk artificial nacre with excellent mechanical properties, Nat. Commun. 8 (2017).
[40] K. Evers, S. Falco, N. Grobert, R.I. Todd, Nacre-like alumina with unique high strain rate capabilities, J. Eur. Ceram. Soc. 40 (2020) 417–426.
[41] Frankberg E J, Kalikka J, García Ferré F, Joly-Pottuz L, Salminen T, Hintikka J, Hokka M, Koneti S, Douillard T, Le Saint B, Kreiml P, Cordill M J, Epicier T, Stauffer D, Vanazzi M, Roiban L, Akola J, Di Fonzo F, Levänen E and Masenelli-Varlot K Highly Ductile Amorphous Oxide at Room Temperature and High Strain Rate.
[42] S. Deville, Freeze-casting of porous ceramics: a review of current achievements and issues, Adv. Eng. Mater. 10 (2008) 155–169.
[43] P.Y. Chen, J. McKittrick, M.A. Meyers, Biological materials: functional adaptations and bioinspired designs, Prog. Mater. Sci. 57 (2012) 1492–1704.
[44] A.M. Abazari, S.M. Safavi, G. Rezazadeh, L.G. Villanueva, Modelling the size effects on the mechanical properties of micro/nano structures, Sensors (Switzerland) 15 (2015) 28543–28562.
[45] Y.Y. Tsai, S.W. Chang, Size effects of mechanical properties of nanohoneycomb with multiple surface orientations, Mech. Mater. 165 (2022).
[46] J. Besson, J. Besson, Continuum models of ductile fracture : a review, Int. J. Damage Mech. 19 (2010) 3–52.
[47] K. Niihara, R. Morena, D.P.H. Hasselman, Evaluation of 1Kic of Brittle Solids by the Indentation Method with Low crack-to-indent Ratios, 1982.
[48] Seyed Mohammad Mirkhalaf Valashani and Francois Barthelat, A laser-engraved glass duplicating the structure, mechanics and performance of natural nacre, Bioinspir Biomim 10 (2015) 026005.
[49] O.T. Picot, V.G. Rocha, C. Ferraro, N. Ni, E. D'Elia, S. Meille, J. Chevalier, T. Saunders, T. Peijs, M.J. Reece, E. Saiz, Using graphene networks to build bioinspired self-monitoring ceramics, Nat. Commun. 8 (2017).
[50] J. Huang, S. Daryadel, M. Minary-Jolandan, Low-cost manufacturing of metal-ceramic composites through electrodeposition of metal into ceramic scaffold, ACS Appl. Mater. Interfaces 11 (2019) 4364–4372.
[51] J. Huang, W.S. Rubink, H. Lide, T.W. Scharf, R. Banerjee, M. Minary-Jolandan, Alumina–nickel composite processed via Co-Assembly using freeze-casting and spark plasma sintering, Adv. Eng. Mater. 21 (2019).
[52] G. Dwivedi, K. Flynn, M. Resnick, S. Sampath, A. Gouldstone, Bioinspired hybrid materials from spray-formed ceramic templates, Adv. Mater. 27 (2015) 3073–3078.